Spring 2015

Phenomenology of a Toy Model Inspired by the Spontaneous Reduction of the Spectral Dimension in Quantum Gravity

Patrick A. Greene
University of New Hampshire, Durham, pan56@unh.edu

Phenomenology of a Toy Model Inspired by the Spontaneous Reduction of the Spectral Dimension in Quantum Gravity

Patrick Greene
(Dated: December 12, 2016)

Attempts to formulate a quantum theory of gravity have generated many sophisticated models. Though fundamentally different, they necessarily exhibit behaviors resembling experimental observations and standard theoretical expectations. Often, their similarities go no further. However many models unexpectedly predict a change in the spectral dimension of spacetime at very small scales (See [1] and references therein for examples). In particular, some of the models predict the spectral dimension changes from 4 to 2. This paper investigates the phenomenological consequences of a toy model that use Planck-scale 2D hypersurfaces, specifically triangles, embedded in 4D Minkowski spacetime. We randomly generated sequences of triangles that a particle might traverse if the distribution of triangles were Lorentz invariant, and we find that triangles further in the sequence tend to differ from those earlier, causing the spectral dimension to grow past 4 for sequences of many triangles. In so doing, we have shown that any method which uniformly fills 4D space with connected 2D triangles with Gaussian distributed proper lengths and causal paths cannot be Lorentz invariant.

I. INTRODUCTION

Although quantum field theory accounts for three of the four fundamental forces, it fails when applied naturally to gravity. One of the great challenges of modern theoretical physics has been to create a complete quantum theory of gravity. The many attempts include string theory [8], loop quantum gravity [6], causal dynamical triangulations (CDT) [5], causal set theory (CST) [4], and Horava-Lifshitz gravity [2]. Theoretical models of quantum gravity are often incredibly complex and difficult to work with, in which case it is advantageous to study simplified toy models, as we do here. Although they do not form a complete representation of a theory, toy models can be used to examine some of its particular limitations and properties, and thus guide the development of more complete theories. Much of the work in quantum gravity centers on evaluating these theoretical models for both familiar familiar behaviors which have been experimentally tested and new behaviors that could be experimentally tested. For example, all theoretical models of quantum gravity are required to be Lorentz invariant up to experimental bounds. Translational symmetry is also expected properties of well-behaved models.

An unexpected emergent property shared by several popular models of quantum gravity has surfaced in the past decade: the *spectral dimension* of spacetime changes at very small scales, generically assumed to be of order the Planck length. In particular, in some of the models the spectral dimension reduces from 4 to 2. The spectral dimension characterizes the return probability when undergoing a random walk; a particle random walking along a line will be far more likely to have returned to the origin after a given number of steps than a particle on a plane. In flat spaces[1] and ordinary random processes, the spectral dimension and the Hausdorff dimension agree[2] however there are some cases in which they differ, such as with fractals or space-times whose curvature is the same scale as the step size. In many of the models mentioned above, the Hausdorff dimension is not even well defined, so the spectral dimension is used instead.

In this paper we will consider a discrete model of quantum gravity in which the Hausdorff dimension is well defined at very small scales, and furthermore agrees with the spectral dimension of 2. In other words, a model in which spacetime is fundamentally constructed of two dimensional hypersurfaces, which fill the 4D spacetime. Discrete models of quantum gravity, such as CST, CDT, and LQG, frequently show interesting behavior regarding Lorentz Invariance. We will therefore propose a "simplest" toy model with which we will explore the implications of a discrete Lorentz Invariant fundamentally 2D model of quantum gravity.

---

[1] More generally, on spaces which are approximately flat over the characteristic step length in the random walk.
[2] The Hausdorff dimension is the typical sense of dimension

II. BACKGROUND

A basic understanding of a fairly wide range of topics is applied in this paper. As a first exploration of this new model of quantum gravity, our goal has been to apply the simplest mathematical tools and making the simplest assumptions, while still acquiring valuable results. In particular, it is necessary to have a basic understanding of special relativity, discrete models of quantum gravity, and the interpretation of the spectral dimension.

A. Special Relativity, Metrics, and Minkowski Space

Einstein founded special relativity on the two axioms that basic physical properties are the same in all inertial frames and that the speed of light c is such a constant physical quantity. From this, he showed that physics is fundamentally unchanged by Lorentz transformations, which allow the observations of relatively moving observers to be reconciled. This symmetry, referred to as Lorentz Invariance, has been extensively tested experimentally through both terrestrial and astronomical observations [3]. In the same way that universal theory must obey rotational and translational symmetry, any well-formulated theory of quantum theory must at least satisfy these experimental constraints, if not exact Lorentz Invariance.

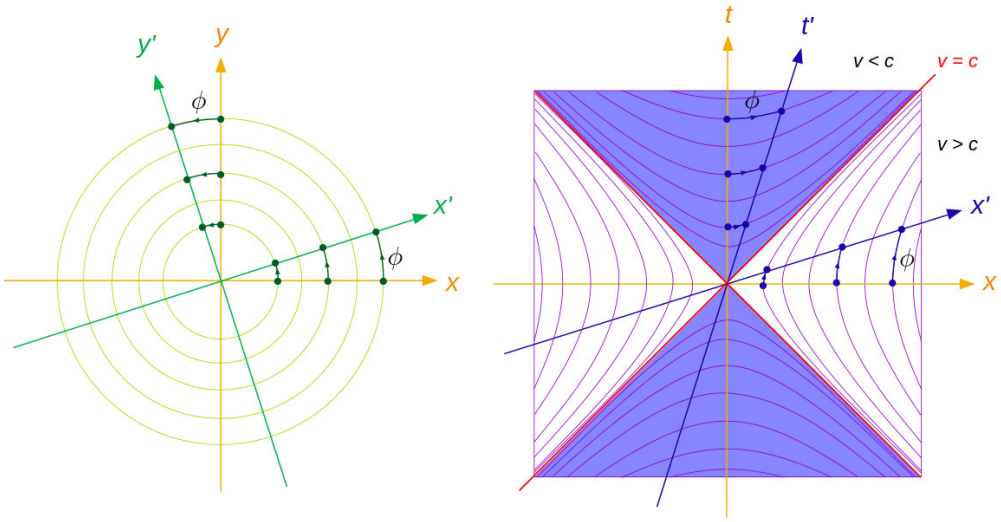

FIG. 1: A representative graph of rotations (left) and Lorentz Transformations (right), both showing a transformed frame of reference. In the image at right, the blue shaded regions are time-like and the unshaded regions are space-like. A vector in the time-like regions will always be time-like, and likewise for vectors in the space-like regions. Image Source: Wikipedia

Lorentz transformations can be thought of as generalized rotations between space and time, except that rather than shifting displacements around a circle, Lorentz transformations shift displacements along hyperbolae, as shown in Figure 1. This means that a vector which begins in the time direction cannot be transformed such that it is in a spatial direction. There is thus a rigid distinction between time-like vectors, which can be transformed until they point in the purely time direction and lie in the shaded regions in Figure 1, and space-like vectors, which can be transformed until they point in a purely spatial direction and lie in the unshaded regions. The boundary between these two regions corresponds to the speed of light, or to null rays, to which the aforementioned hyperbolae approach asymptotically. An important difference between rotations and Lorentz transformations is that the set of possible distinct rotations is bounded between 0 and 2π whereas the set of Lorentz transformations is not bounded.

Related to these transformations is the concept of the squared proper length s^2 as a dot product of a four-vector $v^\mu = (t, x, y, z)$ with itself, where the dot product is defined as

$$s^2 = v^\mu g_{\mu\nu} v^\nu$$

where

$$g_{\mu\nu} = \begin{pmatrix} -1 & 0 & 0 & 0 \\ 0 & 1 & 0 & 0 \\ 0 & 0 & 1 & 0 \\ 0 & 0 & 0 & 1 \end{pmatrix},$$

is the metric of the spacetime. Note that we have, without loss of generality, assumed that the speed of light $c = 1$. The metric determines the behavior of the spacetime, and in General Relativity, gravity is characterized by changes in the metric. The above metric, called the Minkowski metric applies for flat spacetimes with no gravitational effects. In addition to characterizing the proper length in a space, the metric also implies a characteristic volume of that spacetime. For any dimensional space, the unit volume on that space is given by

$$V = \sqrt{|\det g_{\mu\nu}|}.$$

For example, the unit of four-volume for the Minkowski metric is simply 1.

B. Discrete Quantum Gravity

Quantum mechanics, which has failed to fully incorporate general relativity, is often characterized by discrete observable quantities. On the other hand, general relativity accounts for gravity as a warping of space and time. It is thus natural that some theoretical models of quantum gravity should discretize spacetime, that is to say break spacetime into microscopic bits. Such models include CDT, CST, and loop quantum gravity. In these models, the smooth and continuous 4D spacetime we observe in everyday life is an emergent phenomenon. In these discrete models of quantum gravity, the spacetime is often broken into pieces that are not themselves 4D, but fill the 4D space in the same sense that a 1D strand of yarn fills a 3D ball.

The spacetime in CST is constructed from 1D causal links between points. Space-time is filled with these points using a Poisson distribution. This method of filling spacetime is not exactly Lorentz Invariant for a finite number of points. The spacetime in CDT is constructed from 3D simplices, both of which are embedded in 4D spacetime, but is generated dynamically as a particle propagates and studied using Monte-Carlo simulations. In this paper, we will consider a discrete model which is fundamentally 2D, which although initially inspired by the reduction in the spectral dimension in other models, also neatly fills the gap between CST and CDT. Like CST and CDT, we will require that every hyper-surface has at least one time-like side. This guarantees that standard particle propagation can occur on every surface. Also like the other models, we will require that the surfaces be Planck scale.

A fundamental problem with discrete models of quantum gravity centers on Lorentz Invariance. Recall that the curve which represents Lorentz Transformations, as a circle does rotations, is a hyperbola. For a distribution of discrete quantities of spacetime to be Lorentz Invariant, they would need to be distributed uniformly along the hyperbola. Unfortunately, that places an infinite number of those quantities at nearly null displacements in any given frame. These very boosted features would be macroscopically observable. This is the particular behavior we seek to explore in our exploration of this model.

C. Spectral Dimension

The spectral dimension is a quantity which characterizes the return probability as a function of the number of iterations of a Weiner process (essentially a random walk). For example, if you perform a random walk

with equal step sizes on a 1D line, then after the first step, there is a 1/2 chance of returning to the origin, but if this were performed on a 2D lattice, the return probability would be 1/4, and for a 3D lattice it would be 1/6, and so on. In general, after n iterations in dimension d_s,

$$P_n \sim n^{-d_s/2}, \tag{1}$$

where P_n is the probability of a return after n iterations. Given the probabilities P_n, then we can find d_s from

$$d_s = -2\frac{\partial \log(P_n)}{\partial \log(n)}. \tag{2}$$

This says that the spectral dimension is proportional to the slope of the log-log curve for the return probability as a function of iteration[3] . For a smooth spacetime, this would be constant. For the purposes of this paper, because we will be working with discrete data, we will approximate the derivative using linear regression on segments of the log-log curve.

The spectral dimension is important in studies of quantum gravity because in many cases the typical Hausdorff dimension is not well defined. Even when the Hausdorff dimension is well defined, it does not always agree with the spectral dimension, which can be an indication of fractal structure, or other intriguing properties of the space.

III. CHOOSING A MODEL

We want to clearly formulate the simplest means to explore a model which fills 4D spacetime with 2D surfaces while ideally preserving rotational, translational, and Lorentz symmetries, described above. The simplest way to fill 4D spacetime with 2D surfaces is with a uniform grid, however this would unavoidably violate the Lorentz symmetry a uniform grid is only uniform in a particular frame. Furthermore, any spherically symmetric grid would violate translational symmetry, and any translationally symmetric grid would violate rotational symmetry. We are thus restricted to considering random grids of 2D surfaces. Any method for exploring this model must therefore be random in nature. Ideally, the distributions of the characteristic properties of the surfaces must be Lorentz invariant, as well as translationally and rotationally invariant, however wherever there may be a conflict, in this paper we will prioritize Lorentz Invariance. As mentioned, we will also require that every surface contain a causal path, allowing for a straight-forward conceptualization of trajectories and a guarantee of causality.

Towards our goal of seeking the simplest model, we will use the simplest 2D surfaces, namely triangles. Using simplices also follows the example of CDT, which as its name suggests uses 3D simplices, commonly referred to as tetrahedra. We must consider how the triangles are glued together such that they fill 4D space while preserving the aforementioned symmetries at large scales. It is not a simple task to lay down such spacetime all at once, in the way that CST does. However our goal is merely to estimate the spectral dimension and distribution of triangles random walk trajectories in the spacetime, which does not require that we have the entire space all at once. Whenever a trajectory reaches the edge of a triangle, it will pass onto a new triangle. If the overall distribution of triangles is Lorentz invariant, then the new triangle must be chosen from a Lorentz invariant distribution. Therefore, we can explore the properties of a spacetime filled with 2D triangle by generating sequences of triangles, each off of a randomly selected edge of another in a Lorentz invariant manner.

We will perform Monte-Carlo simulations, generating many sequences of triangles. Because we are not tracking an actual particle, we will say a sequence of triangles has "returned" when the center of the last triangle is within one proper Planck length of the origin. The return probability may then be calculated as

---

[3] Note that any base of logarithm will work for this purpose.

the number of triangles in each iteration that have returned, out of all the runs. The spectral dimension can then be calculated from using Equation 2. We will then evaluate whether the spectral dimension converges to four after many iterations. We will also evaluate whether the triangles remain translationally and rotationally invariant, as these are not strictly imposed by our method. In particular, because we are generating from a triangle at a particular point, translational invariance would seem particularly endangered. In addition, because this method is intended to represent a sequence of triangles in a uniform spacetime, there is an expected sequential symmetry, meaning that the distributions and properties of triangles remain unchanged along a sequence.

There are some noteworthy details regarding our proposed method. Notice that we are not actually observing trajectories directly, but rather inferring their behavior through making random guesses, which greatly simplifies the computational work. As a result of this simplification, it cannot be expected that the spectral dimension we calculate will be 2 at small scales. Note also that we are imposing no requirements that the triangles not intersect, again to simplify computation. It is unclear what if any effects this may have on our results. Last of all, we will assume there are only two triangles on each edge, so that if the trajectory doubles back, it must return to the previous triangle. Otherwise edges earlier in the sequence will tend to have far more triangles than those later in the sequence.

IV. DERIVATION OF OUR METHOD FOR GENERATING TRIANGLES

In this section, we work through the details of our Lorentz invariant method for generating a new triangle from a randomly selected side of an old triangle. At least three four-vectors are required to fully characterize a triangle. For our purposes, the simplest way is to use two vectors with a common origin, which is itself given by a third vector. Thus each new triangle can be generated off of an old triangle by adding a new side which is generated in a Lorentz invariant manner which also guarantees the new triangle is from the same distribution as the first. The third side of the triangle is of course implied as the vector connecting the other two sides. Given the two sides, a_1^μ and a_2^μ, and the origin, b^μ, the 3rd side is given by

$$a_3^\mu = a_2^\mu - a_1^\mu,\ b_3^\mu = a_1^\mu + b^\mu.$$

However, because we are not choosing this side directly, we must be careful that the distribution of third sides be indistinguishable from the distribution of the first and second sides.

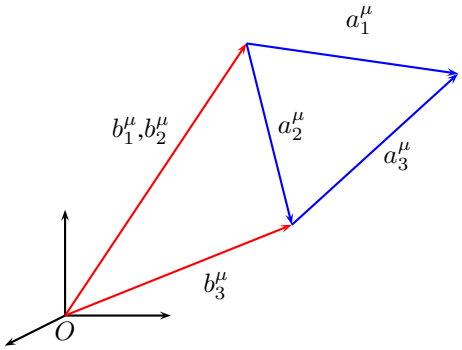

Another key property of the triangle is its area. because the triangles are embedded in 4D spacetime, the Euclidean formula for calculating the area will not generally hold. However, recall that the generalized volume of a space can be found from the determinant of the metric. The generalized volume of a 2D surface is its area. So, to determine the area, we calculate the *induced metric*, which is the metric for vectors defined on an embedded surface,

$$h_{ij} = a_i^\mu g_{\mu\nu} a_j^\nu, \tag{3}$$

where i and j are either 1 or 2, corresponding to either side 1 or side 2. The area A is then given by

$$A = \frac{1}{2}\sqrt{|\det(h_{ij})|}. \tag{4}$$

I will also define a shorthand notation for the Minkowski dot product of any two sides:

$$\lambda_{ij} = a_i^\mu g_{\mu\nu} a_j^\nu,$$

where i and j may here be 1, 2, or 3. Note that the induced metric is a subset of the possible λ_{ij}'s.

Each new side vector could be generated by boosting a unit time or space vector by a random rapidity, which is essentially the angle for a Lorentz transformation. Unlike an angle where the value is restricted to the interval of 0 to 2π, a Lorentz invariant rapidity would be randomly selected from $-\infty$ to $+\infty$, with every value carrying an equal probability. This poses two problems: One, normalization is awkward, and two, this would result in almost all sides being nearly null, as described above, making all the triangle more like shards, and particles would be forced to move along them for macroscopic distances. If this were the case, it would have been observed. However we also have the constraint that the sides meet to form a triangle and that the distributions of sides be indistinguishable.

A. The system of equations

The randomly selected spacial coordinates will necessarily have a limited magnitude due to the nature of random number generators. In addition, computational limits aside, we want to impose a proper-length condition on the sides and we also want to have some control of the area. We could require that every side have the same proper length l, which would also determine the area. Alternatively, we might limit the area, and from that find limits on the selection of our sides. The area A is given by Equation 4, which can be expanded in terms of the induced metric to give

$$A = \frac{1}{2}\sqrt{|h_{11}h_{22} - (h_{12})^2|} = \frac{1}{2}\sqrt{|\lambda_{11}\lambda_{22} - (\lambda_{12})^2|}. \tag{5}$$

Because we cannot (computationally) select a value from an unbounded set, we will select l_1, l_2, and l_3 from a Gaussian distribution[4] centered at the Planck length, which we will without loss of generality set equal to 1. Thus the area will be of order the Planck Lengths squared.

As stipulated, the third side must be indistinguishable from the other sides. Using the fact that the vector for the third side is the difference of the other two side vectors, its squared proper length is

$$\begin{aligned}\lambda_{33} &= (a_2 - a_1)^\mu g_{\mu\nu}(a_2 - a_1)^\nu \\ &= a_1^\mu g_{\mu\nu} a_1^\nu - 2a_1^\mu g_{\mu\nu} a_2^\nu + a_2^\mu g_{\mu\nu} a_2^\nu \\ &= \lambda_{11} - 2\lambda_{12} + \lambda_{22},\end{aligned}$$

where we have again used the λ_{ij} notation for brevity. Isolating the λ_{12} term, we find

$$\frac{1}{2}(\lambda_{11} + \lambda_{22} - \lambda_{33}) = \lambda_{12}, \tag{6}$$

and substituting into Equation 5, we get a relation strictly between the area and the proper lengths:

$$A = \frac{1}{2}\sqrt{\lambda_{11}\lambda_{22} - [(\lambda_{11} + \lambda_{22} - \lambda_{33})/2]^2}$$

---

[4] Yes, this is still technically unbounded, but one might call it *practically* bounded, because the most likely values are all in a finite region.

which simplifies to

$$A = \frac{1}{4}\sqrt{|2(\lambda_{11}\lambda_{22} + \lambda_{11}\lambda_{33} + \lambda_{22}\lambda_{33}) - (\lambda_{11}^2 + \lambda_{22}^2 + \lambda_{33}^2)|}. \tag{7}$$

This shows that constraining the area and any two sides is the same as constraining all three sides. If we select λ_{11} and λ_{22} from a particular distribution, and then select λ_{33} such that A is constant, λ_{33} will have a different distribution that the other two sides. This can be clearly seen in Figure 2. The distribution of

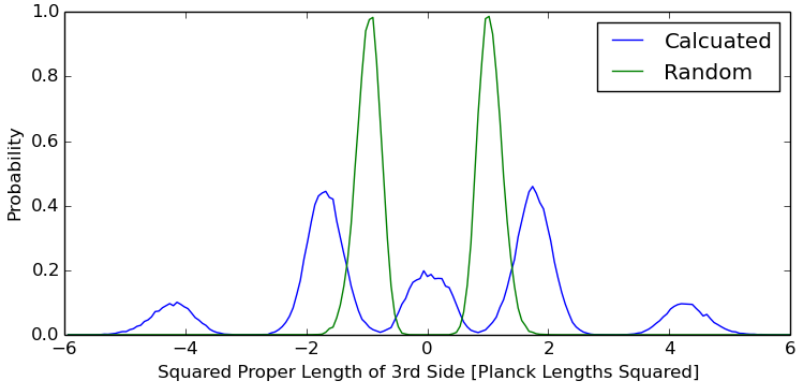

FIG. 2: The distributions of λ_{33} when selected from a Gaussian distribution like the other two sides, and when it is calculated by choosing the other two sides from the Gaussian and then imposing that $A = 1$. Note that the third sides would be clearly distinguishable from the other sides. In both cases, the center of the Gaussian was 1.0 and the standard deviation was 0.05.

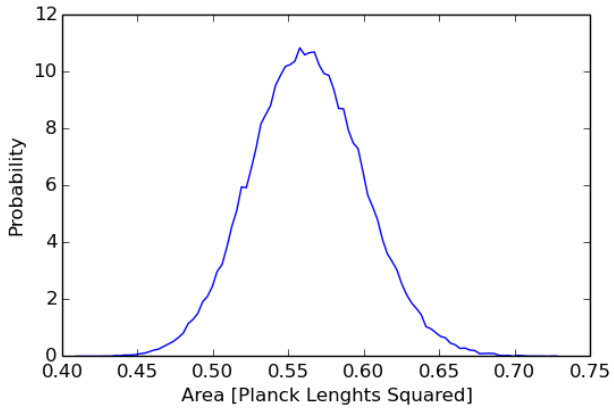

FIG. 3: The distribution of areas from choosing the λ_{ii}'s randomly

areas, given that all the squared proper lengths of the sides are selected from the same distribution, shown in Figure 3.

B. Deriving The Algorithm

For all but the first triangle, we will begin with one side already defined. The proper lengths of the other two sides will then be randomly selected from a Gaussian distribution centered at one. For the first triangle we will, without loss of generality, choose the first side as either in the t direction or the x direction, with the length randomly chosen as described above[5] . One may recall that in Cartesian space it is not in general possible to create a triangle from three sides with arbitrary lengths, specifically if the sum of the lengths of two of the sides is less than the third. However this is **not** true for Minkowski space. The difference can be seen in Equation 6: in Cartesian space, the dot product (λ_{12}) would be positive definite. Thus, if $\lambda_{11} + \lambda_{22}$ was less than λ_{33} (recalling that these quantities would also be positive definite), there would be a contradiction. But the dot product in Minkowski space is **not** positive definite, therefore no matter the side lengths, there is no contradiction, therefore we can choose any side lengths (that is, *proper lengths*) we want and still get a triangle. There will however be some constraints on whether the sides are space-like or time-like. This must be the case because 3D Euclidean space is a subset of Minkowski space, specifically where $t = 0$. In this case the squared proper lengths are the squared lengths, and the ordinary restrictions would then apply.

Thus, we will choose or begin with λ_{11}, λ_{22}, λ_{33}, t_1, r_1, θ_1, and ϕ_1. We will then essentially choose θ_2 and ϕ_2 from some bounded interval which is not necessarily $-\pi$ to π. Equation 6 can be rewritten

$$\lambda_{12} = -t_1 t_2 + r_1 r_2 \cos\psi, \tag{8}$$

where

$$\begin{aligned}\cos\psi = &\cos\theta_1 \cos\theta_2 \cos\phi_1 \cos\phi_2 \\ &+ \cos\theta_1 \cos\theta_2 \sin\phi_1 \sin\phi_2 \\ &+ \sin\theta_1 \sin\theta_2\end{aligned}$$

is the cosine of the angle between the spacial components of the two sides. This equation can be solved for t_2 and r_2 to give

$$t_2 = \frac{\lambda_{12} t_1 \pm r_1 \cos\psi \sqrt{\lambda_{12}^2 - \lambda_{22}(-t_1^2 + r_1^2 \cos^2\psi)}}{-t_1^2 + r_1^2 \cos^2\psi} \tag{9}$$

$$r_2 = \frac{\lambda_{12} r_1 \cos\psi \pm t_1 \sqrt{\lambda_{12}^2 - \lambda_{22}(-t_1^2 + r_1^2 \cos^2\psi)}}{-t_1^2 + r_1^2 \cos^2\psi}. \tag{10}$$

Because we cannot have complex radii or times, we will require that radicand be non-negative:

$$\lambda_{12}^2 - \lambda_{22}(-t_1^2 + r_1^2 \cos^2\psi) \geq 0 \tag{11}$$

This will place some constraints on our choice of the squared proper lengths of the sides, and in some cases ψ (and consequently θ_2 and ϕ_2). There are several cases to consider, specifically depending on whether $r_1 = 0$ or not, and the sign of λ_{22}.

Let us first consider the case in which $r_1 = 0$, then $-t_1^2 = \lambda_{11}$, so inequality 11 becomes

$$\boxed{\lambda_{12}^2 - \lambda_{22}\lambda_{11} = -\det(h_{ij}) \geq 0.} \tag{12}$$

It is noteworthy that the result indicates that the negative of the determinant of the induced metric is non-negative. Let us now consider the case where $r_1 \neq 0$, and thus $\cos^2\psi$ does not drop out. By definition,

---

[5] This is exactly identical to the process for the other sides, because we can always Lorentz boost and rotate to either t or x.

$\cos^2\psi$ ranges between 0 and 1, so the λ's must be chosen such that this is not violated. Solving inequality 11 for $\cos^2\psi$, and taking consideration for the sign of λ_{22}, because if $\lambda_{22} < 0$, the sign of the inequality would need to be swapped when multiplying or dividing by λ_{22}, we find

$$\cos^2\psi \leq \frac{\lambda_{12}^2 + \lambda_{22}t_1^2}{\lambda_{22}r_1^2}, \text{ for } \lambda_{22} > 0 \tag{13}$$

$$\cos^2\psi \geq \frac{\lambda_{12}^2 + \lambda_{22}t_1^2}{\lambda_{22}r_1^2}, \text{ for } \lambda_{22} < 0 \tag{14}$$

Note that as r_1 approaches 0, the top equation approaches positive infinity, in which case there is no constrain on ψ, consistent with our earlier analysis. At the same time, the bottom equation approaches negative infinity. To see this, recall that although the numerator may in general be negative, we already showed that at $r_1 = 0$, that expression must be greater than or equal to zero, and thus non-negative. Therefore, because the denominator is negative (recalling that $\lambda_{22} < 0$), the expression approaches negative infinity, and again there is no constraint on ψ.

If $\lambda_{22} > 0$, then to avoid any constraints on ψ, thereby guaranteeing rotational symmetry,

$$\frac{\lambda_{12}^2 + \lambda_{22}t_1^2}{\lambda_{22}r_1^2} \geq 1,$$

which, when solved, again gives inequality 12. This constraint is not a minimal constraint for the system of equations to be solvable. So long as

$$\frac{\lambda_{12}^2 + \lambda_{22}t_1^2}{\lambda_{22}r_1^2} \geq 0,$$

there would be no contradiction. We thus have a choice between two constraints. If $\lambda_{22} < 0$, it appears there may be a problem, because the right hand side of inequality 14 may be greater than one. Thus it is *necessary* that

$$\frac{\lambda_{12}^2 + \lambda_{22}t_1^2}{\lambda_{22}r_1^2} \leq 1,$$

which again leads to inequality 12.[6] However this leaves a constraint on ψ. To avoid that constraint, it would be necessary to impose that

$$\frac{\lambda_{12}^2 + \lambda_{22}t_1^2}{\lambda_{22}r_1^2} \leq 0,$$

which, because $\lambda_{22} < 0$ implies that

$$\lambda_{12}^2 + \lambda_{22}t_1^2 \geq 0.$$

Again we have a choice between two constraints, a stronger and a weaker, however this time the one related to Inequality 12 requires breaking rotational symmetry, while the other constraint does not.

Case	Minimum Requirement	Rotational Symmetry
$\lambda_{22} > 0$	$\lambda_{12}^2 + \lambda_{22}t_1^2 \geq 0$	$-\det(h_{AB}) \geq 0$
$\lambda_{22} < 0$	$-\det(h_{AB}) \geq 0$	$\lambda_{12}^2 + \lambda_{22}t_1^2 \geq 0$

TABLE I: Summary of the constraints to create a triangle.

[6] again, taking care with the sign of λ_{22} and the inequality

This in fact a choice between maintaining the indistinguishability of the sides and rotational invariance. To enforce the rotational symmetry constraint when $\lambda_{22} < 0$, recall from Equation 6 that

$$\lambda_{12} = \frac{1}{2}(\lambda_{11} + \lambda_{22} - \lambda_{33}).$$

By our method of selection, λ_{11} and t_1 are already known. Thus this equation in addition to our constraining equation gives

$$\lambda_{11}^2 + \lambda_{22}^2 + \lambda_{33}^2 + 2\lambda_{22}(r_1^2 + t_1^2) - 2\lambda_{11}(\lambda_{22} + \lambda_{33}) \geq 0,$$

which means we can choose either λ_{22} or λ_{33}, then solve for the allowable range for the other, and select from said range. Note that the indexing of the variables is very much not arbitrary, meaning that the sides are mathematically distinguishable, which violates one of our fundamental requirements. The same is true if we only impose the minimum requirement for $\lambda_{22} > 0$. We therefore require that $-\det(h_{AB}) \geq 0$. We will see that this constraint can be met naturally by requiring that there is a causal path along every triangle.

Recall that in Minkowski space, as state earlier, there are no constraints on the squared proper lengths of the sides of a triangle, but that there could be constraints on their signs, which is equivalent to controlling whether they are time-like or space-like. Inequality 12 provides those constraints. First, recall that Inequality 12 can also be written

$$\lambda_{11}^2 + \lambda_{22}^2 + \lambda_{33}^2 - 2(\lambda_{11}\lambda_{22} + \lambda_{11}\lambda_{33} + \lambda_{22}\lambda_{33}) \geq 0 \tag{15}$$

If the squared proper lengths were all the same sign, Inequality 12 could be violated. For example, consider the case where $\lambda_{11} = \lambda_{22} = \lambda_{33} = 1$ (recalling that Planck length is 1). The value of the left hand side would be -3, violating the inequality. The same is true if all the squared proper lengths were -1.

If, however, one of the squared proper lengths has a different sign, then the inequality is *always* satisfied. Suppose λ_{33} were negative, and the rest were all positive. The left hand side of Equation 15 would have the form

$$a^2 + b^2 + c^2 - 2ab + 2ac + 2bc = (a-b)^2 + c^2 + 2(a+b)c, \tag{16}$$

where a, b, and c **are all positive**. Now suppose the above expression is in fact less than zero, thus violating the inequality. The first and second terms are both positive definite, and $(a+b)$ is also positive, because a and b are each positive by hypothesis. Thus the only way that the expression could be negative is if c were negative, but like a and b, c must be positive. Thus there is no way for the expression to be negative if λ_{33} is the only negative squared proper length. The same is true if λ_{11} or λ_{22} are the only negative squared proper length, because the labelling of the λ_{ii}'s is arbitrary. We again have the same result if only one squared proper length is positive and the rest are negative. The resulting expression is identical to Equation 16. Thus, when making a choice in the sign of the squared proper lengths, there are only six possibilities that are guaranteed to obey Equation 12:

$$(-,-,+), (-,+,-), (+,-,-), (-,+,+), (+,-,+), (+,+,-) \tag{17}$$

where, for example, $(-,-,+)$ means λ_{11} and λ_{22} are negative, and λ_{33} is positive. The sign of the first side will be given, so we will randomly choose one of the three remaining viable options to determine the signs of the other two sides.

Therefore we now have the means to choose ψ in a consistent manner. There is a remaining degree of freedom which is equivalent to a rotation about the spacial component of the first side. The most natural choice would be to randomly select this angle, ξ, on the interval from $-\pi$ to π. We will then rotate the vector defined in terms of ψ and ξ around the x and z axes by θ_1 and ϕ_1, respectively. Note that triangles can be generated into the past. This does not mean that we are imagining particles propagating back in time, but rather that we are considering alternative paths that particles might have taken to reach a particular triangle. This is an essential part of measuring the spectral dimension.

V. OUR MONTE-CARLO SIMULATIONS

In this study, we applied Monte-Carlo methods to explore the limitations on filling 4D spacetime with 2D triangles by tracing the path of a particle from triangle to triangle, generating each new triangle in a Lorentz Invariant manner.

A. Applying the Algorithm

The algorithm was applied using an object oriented framework in Python[7]. At the lowest level, there are Vector, Side, and Triangle classes. The algorithm for generating new triangles is placed in the initialization of the Triangle class, and the algorithm for generating the first random side is placed in the initialization of the Side class. Each Triangle object holds a list of Side objects, and each Side object holds two vectors corresponding to the origin of the side vector and the side vector itself. All random choices were made using the standard pseudo-random generators available through the numerical python package, and double precision, which is the default for python, was used.

Each simulation was broken into two loops: *runs* and *iterations*. In each iteration, a side is selected randomly and if necessary a new triangle is generated. Iterations correspond to the path of the particle. Each run contains many iterations, approximating the path of the particle from triangle to triangle. Each new triangle is a new generation of triangles. In general, because a particle could backtrack, the generation of the triangle need not correspond to when a particle was on that triangle, that is to say generation and iteration are not the same thing. There is a strong dependence between triangles within the same run, if only because they share sides. However there is no relation between the triangles of different runs, so this would be the level of division ideal for parallel processing, although it was unnecessary in this study to implement it.

At the beginning of a run, we make a random choice between a temporal or spatial 4-vector[8] to be the first side of the first triangle. The length of the vector (which is in this case the same as its proper length) is selected from the same distribution as the other side proper lengths, which for our trials was a Gaussian distribution centered at $1l_P$ (1 Planck Length) with a standard deviation of $0.1l_P$. The second side is then generated using the algorithm described above, with its origin randomly chosen from one of the two endpoints of the first side, such that the proper lengths are all selected from the same distribution, and there is a mixture of time-like and space-like sides. The angles are then selected within the specified bounds, and Equations 9 and 10 are used to solve for t_2 and r_2, respectively. Once the second side is generated, the third side is implied as the difference between the other two side vectors. A side is then selected randomly, and this becomes the first side of a new triangle.

The sign choice is made randomly for most cases, except that null solutions are avoided. The equations should not produce null sides, however the difference may be smaller than numerical precision. There are other points in the calculation that this can occur, so there is also a catch-all in the initialization of a vector object, If at any iteration a null side is caught, the entire run is aborted, and a new run is started. The triangles are largely determined by the squared proper lengths of the sides. Recall that the proper lengths are randomly selected from a Gaussian distribution centered at 1 l_P, so the proper lengths are all about 1. This means that

$$r^2 - t^2 \approx 1.$$

If we define the difference of r and t, $\epsilon = r - t$, then the above becomes

$$(t + \epsilon)^2 - t^2 = 2t\epsilon + \epsilon^2 \approx 1.$$

---

[7] Python was the natural choice for developing the objects. Future projects will likely want to translate the computationally intensive code into C++. The code is designed so that data can be read from a file in a manner that behaves like an ordinary python list, and it is then easy to analyze the data in the ipython –pylab environment

[8] Without loss of generality, we chose x as the default spacial direction.

If $\epsilon << t$, then we can neglect the ϵ^2 term, and we find that

$$\epsilon \approx \frac{1}{2t}. \tag{18}$$

Thus, if r and t are large, the numerical precision to distinguish the two values becomes small, eventually to the point of exceeding numerical precision.

Recall from Equation 1 that there is a proportionality between the return probability and the number of iterations. To have usable statistics up to the last iteration, it is necessary that there be at least one returned triangle at that iteration. The probability P_N of one triangle returning after N iterations is

$$P_N = \frac{1}{M}$$

where M is the number of runs. Using Equation 2 we find that

$$M = N^{d_s/2},$$

where d_s is the spectral dimension[9]. This means that the the computational resources, which correspond directly to the number of triangles T, necessary run the simulation for N iterations goes as

$$T \sim NM = N^{1+d_s/2}. \tag{19}$$

As we will show shortly, this is particularly problematic due to a spectral dimension which increases with iteration.

B. Analyzing the Results

We performed two types of simulation, one in which the particles were assumed to only move forward, so each iteration generated a new triangle, and another in which the particles were allowed to backtrack, so that a particle might end up on the same triangle twice. There were 100,000 runs with 100 iterations each in the first simulation, and 100,000 runs with 200 iterations each in the second simulation. The return probabilities from the simulation of non-backtracking particles are shown in Figure 4a. Note that the slope of the log-log curve is not constant, as would be expected for a flat spacetime, and thus the spectral dimension varies with iteration. We used a linear regression over intervals of log(2) on the log-log plot to estimate the slope of the curve. The fits are also shown in Figure 4a.

The spectral dimensions for non-backtracking particles calculated using Equation 2 are shown in Figure 4b. It is clear that we have failed to achieve a reasonable spectral dimension; after fewer than 20 iterations, the spectral dimension passed 4. Even though the triangles are embedded in 4D space, the rate of decrease in their likelihood of returning appears to more closely correspond to a 9D space after just 60 iterations. This does not of course mean that we are creating a 9D space, it means that the distribution of triangle centers is spreading more quickly than one would expect from a random walk. Recall that in a random walk, each new step must be independent of the previous step. In this case however, the shape of the next triangle is in part determined by the shape of the previous triangle, specifically by the side off of which the triangle spawned. We could not impose any conditions to make the triangles uniform in any given frame because that would break Lorentz Invariance. Figure 5 shows that the average spacial magnitude of the sides of the triangles grows roughly six orders of magnitude over the course of the 50 iterations. This violates the assumption that we are random walking a uniform spacetime, and is the cause for the growth in the spectral dimension.

It is possible, looking at Figure 5 that the average and standard deviation level off after more iterations, so that the non-uniformity is only a transient property, although we do not suspect this is the case. Similarly,

---

[9] Recall that the spectral dimension can be a function of iterations.

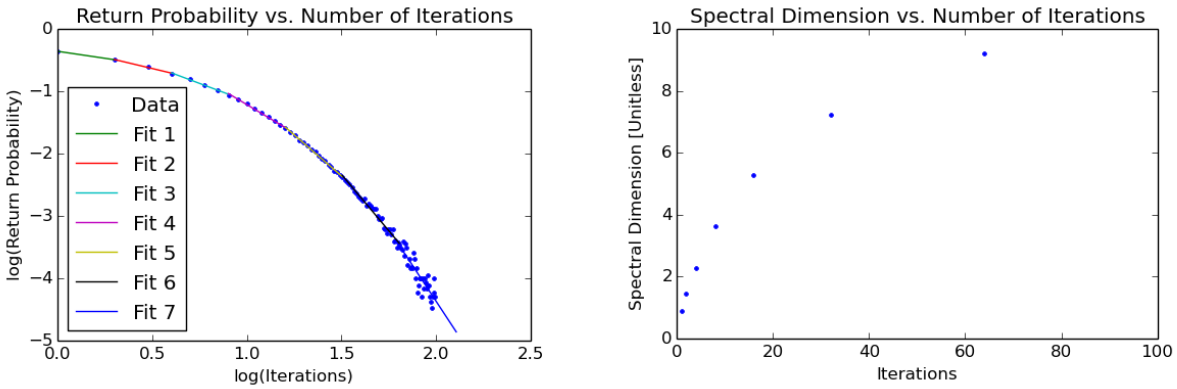

(a) **(b)**

FIG. 4: Plots of the return probability (a) and the spectral dimension (b) as a function of iteration for *non-backtracking* particles. The return probabilities were calculated from the Monte-Carlo simulation. The fits approximating the slope over intervals of log(2). In smooth 4D space, the plot would show a straight line with a slope of -2. The spectral dimension is calculated by applying Equation 2 to the fits shown in (a). Note that after fewer than 20 iterations, the spectral dimension has already exceeded 4.

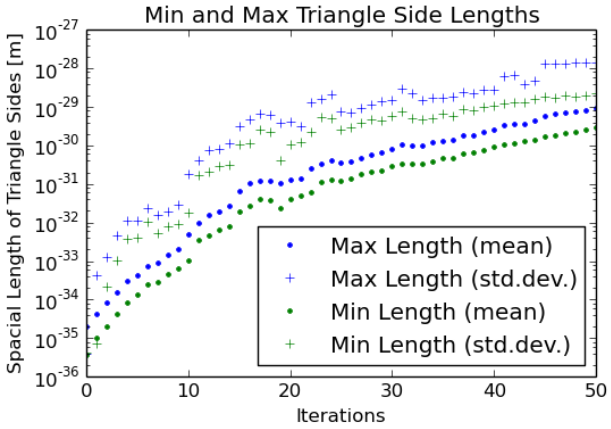

FIG. 5: The mean and standard deviation of the maximum spatial components of the sides with both the shortest and longest spacial components of the triangle at each iteration. Note that the mean spatial component grows between six and seven orders of magnitude, which indicates sharding and nearly null triangles in a particular frame. The large standard deviations indicate that there are many small spacial components and a few very large spacial components.

the spectral dimension may level after more iteration. Unfortunately, it is difficult to probe further. Because the squared proper lengths of the sides are all from the same Gaussian distribution centered on one Planck Length, the increase in the spacial component means that the time component must also be growing rapidly. In other words, the sides of the triangles are on average becoming closer to null with each iteration in the particular frame in which these measurements have been made. This outcome was suspected from the beginning as a result of requiring a Lorentz invariant distribution. The increase in nearly null triangle sides makes it difficult to probe to higher iterations due to the limits of numerical precision highlighted by Equation 18. As an example, by 150 generations, roughly 42% of runs are omitted due to null sides.

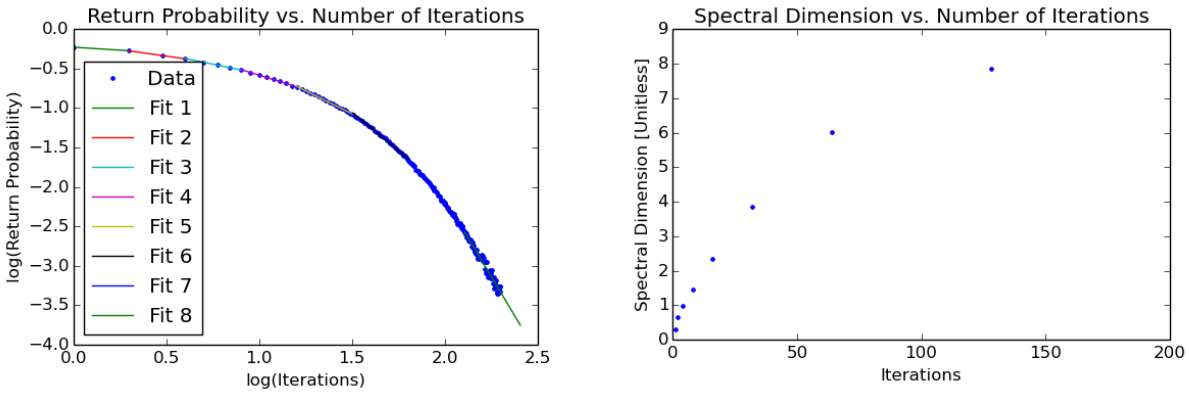

(a) **(b)**

FIG. 6: Similar to Figure 4, plots of the return probability (a) and the spectral dimension (b) as a function of iteration for *backtracking* particles. Note that again the spectral dimension exceeds 4, although it takes many more iterations. This is because the sharding is still a problem, and allowing the particles to go to previous triangles only delays the effect.

Recall that the first side of each triangle (with the exception of the first triangle) is shared with its previous triangle, and that to guarantee that every side is attached to only two triangles, the next triangle could only be generated from one of the other sides. However it was possible that a particle undergoing random walk could return to the previous triangle. This would of course increase the return probability of the particle significantly. This motivated our second simulation of particles that are allowed to backtrack. As shown in Figure 6, the return probability still exceeds 4, although it requires more iterations. This is because backtracking does not avoid the problem that the distribution of triangles become more sharded further from the first triangle, it simply means that the particles do not move away from the first triangle as fast.

VI. CONCLUSIONS AND OPEN QUESTIONS

The Monte-Carlo simulation was proposed to be at least approximately equivalent to exploring a uniform space built from randomly assembled 2D triangles embedded in 4D spacetime in a Lorentz Invariant manner. The algorithm we developed guaranteed that the distribution of triangles would be Lorentz invariant, which determined all but 3 degrees of freedom in the construction of a triangle, given a side. The proper lengths were guaranteed to be uniform, however there were no constraints on the spatial or temporal components of the sides, because any such constraint would risk breaking Lorentz Invariance. Analysis of the simulation has shown that the sides of the triangles inevitably become more sharded more iterations from the first triangle. This led to a spectral dimension larger than would be physically reasonable.

Although allowing the particles to retrace their steps onto previous triangles makes the spectral dimension grow out of control more slowly, the change in the distribution of the lengths of triangles' sides as a function of iteration violates the assumption that the simulation was exploring a uniform space. In Causal Set Theory, the set of points is generated as a whole and then connected. A Poisson distribution is used, which is approximately Lorentz Invariant. This method guarantees a uniform distribution over space. This method might be applicable to a fundamentally 2D space such as the one we consider. However, what we have shown is that if the space is uniform, it cannot be exactly Lorentz invariant. Furthermore, the Poisson distribution violates translational invariance, so even this approach would fail to result in a satisfactory spacetime.

It is possible that the distribution reaches a steady state after more iterations. Unfortunately, the computational limitations discussed above prevented us from exploring this possibility directly. However we suspect

that the sharding is the result of a random walk of the side vectors along the Lorentz Invariant hyperbola, which would mean that the distribution would never truly reach a stead state. A similar effect has been observed in Causal Set Theory [9], where the momentum vectors of a particle grow as a particle diffuses away from the origin. A future project might explore this type of property in a general sense, and seek a mathematical proof that this occurs for building blocks of any dimension embedded in any dimension.

It is worth noting that in both the non-backtracking and backtracking particle simulations, the spectral dimension does not begin as 2. This is because we do not actually track the path of the particle. Naturally, the spectral dimension would be 2, because each triangle is a smooth and flat 2D spacetime. A future project could track actual particles, which would require very little additional work. However, again, this would not eliminate the fact that the triangles become more sharded further from first triangle, and further from the origin the motion of the particle becomes less relevant.

Another more analytic approach to this specific problem would be to use the 2D propagator to estimate the probability of a particle interacting with each side. In this method, the probability is related to the number of ways a particle can move from one point to another along a checkerboard formed form null rays. Although this would not eliminate the problem of sharding, it might produce a more reasonable spectral dimension. This method is guaranteed to be possible because we require causal paths on every triangle, which means there must be null rays on every triangle. Applying any method of calculating the probability of a particle impacting the different sides would be another avenue for future work.

VII. ACKNOWLEDGEMENTS

I would like to give special thanks to David Mattingly, my advisor, who proposed the topic for this project and guided me through the early stages of formulating my approach, and who relentlessly revised both this paper and associated presentations. We would also like to thank Per Berglund for his help in revising this paper. This work was done for my undergraduate honors senior thesis to earn my BS in Physics at the University of New Hampshire, Durham.

---

[1] Carlip, Steven, *Spontaneous Dimension Reduction?*, arXiv, July, 2012
[2] Horava, Petr, *Spectral Dimension of the Universe in Quantum Gravity at a Lifshitz Point*, arXiv, March, 2009
[3] Mattingly, David, *Modern Tests of Lorentz Invariance*, Living Rev. Relativity, 2005
[4] Henson, Joe. *The causal set approach to quantum gravity*, arXiv, January 2006
[5] Ambjorn, J., J. Jurkiewicz, R. Loll *Causal Dynamical Triangulations and the Quest for Quantum Gravity*, arXiv, April 2010
[6] Ashtekar, Abhay, Jerzy Lewandowski. *Background Independent Quantum Gravity: A Status Report* arXiv, September 2004
[7] Moore, D.G., V. H. Satheeshkumar *Spectral Dimension of Bosonic String Theory* arXiv, August 2014
[8] Faraggi, Alon. *String Phenomenology: Past, Present, and Future Perspectives* arXiv, April 2014
[9] F. Dowker, J. Henson and R.D. Sorkin, "Quantum gravity phenomenology, Lorentz invariance and discreteness," Mod. Phys. Lett. A **19**, 1829 (2004) [gr-qc/0311055].